Delevitation Modelling of an Active Magnetic Bearing Supported Rotor

Jan J. Janse van Rensburg[1,a], George van Schoor[1,b], Pieter A. Van Vuuren[1,c]
[1]School of Electrical, Electronic and Computer Engineering North-West University, Potchefstroom, 2520, South-Africa
[a]Jan.JansevanRensburg@nwu.ac.za, [b]George.vanSchoor@nwu.ac.za, [c]Pieter.vanVuuren@nwu.ac.za

Abstract: For active magnetic bearings (AMBs) to be used with confidence in industrial applications, the safe failure of the AMB system should be guaranteed. The exact behaviour of the rotor on the backup bearings (BBs) is relatively uncertain [1,2,3]. Uncertainty in a failure situation means that the safe failure of the AMB system cannot be guaranteed. The purpose of the presented rotor delevitation simulation model (RDSim model) is to eliminate some of the uncertainties associated with a rotor delevitation event.
The simulation model includes a flexible rotor model [4], a non-linear AMB model [5], a non-linear BB model, stator effects, active rotor braking, rotor free running, inner race speed up, AMB/BB load sharing and sudden unbalance (blade-loss simulation). The RDSim model can be used to simulate any AMB failure on one or more locations. The failure modes include power amplifier (PA) malfunction, AMB coil short-circuit, total power failure and controller failure.
This paper will discuss the BBSim model; a brief explanation of each of the sub-models of the BBSim model is also given.

Keywords: Backup Bearings, Auxiliary Bearings, Rotordynamics, Active Magnetic Bearing, Modelling, Simulation, Transient, Rotor Delevitation

1. Introduction

The greatest safety risk during an AMB failure is the development of backward whirl. This causes very large forces on the BBs and almost certainly the failure of the BB. In order to avoid backward whirl the cause first needs to be fully understood. The RDSim model can be used to determine the causes of whirling and recommendations can be made to avoid it.

Forward whirling may be attributed to high braking torque applied to the rotor during an AMB failure in conjunction with other exaggerating effects as mentioned in previous research [6,7,8,9].

The transient forces experienced by the BBs during an AMB failure event are crucial in determining the lifespan of the BB. The ability to determine the maximum force that the BB will experience enables optimum bearing selection.

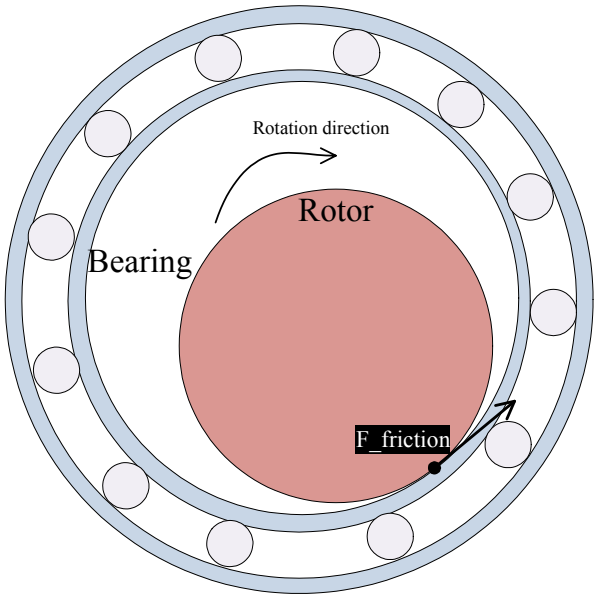

Fig. 1: Model summary (Rotational)

Based on the comparison of the simulation and experimental results performed on a 4-axis AMB suspended flexible rotor [10] and a 5 axis AMB suspended rotor [11] the efficacy of the BBSim model is evaluated. The BBSim model could be used to make BB design recommendations, relating the maximum transient force and the maximum acceleration that

the BB will experience. The BBSim could also be used to predict the occurrence of forward and backward whirling and the associated forces.

2. The backup bearing simulation (BBSim)

The developed BBSim model consists of four main sub-models: a rotor-model, AMB-models, BB/stator-models (translational and rotational). The rotational BB and Stator model is shown in Fig.1 and the three translational sub-models are shown in Fig. 2.

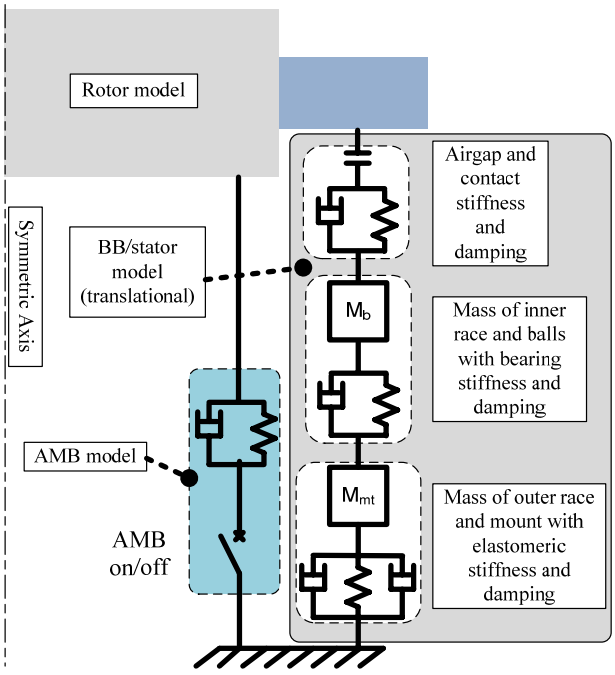

Fig. 2: Model summary (Translational)

2.1. Airgap and contact modelling.

The airgap can be defined as a span of co-ordinates in which there is no force acting on the rotor. Should the airgap be exceeded the normal differential equations are valid. The air-gap cannot be represented with constants in an orthogonal co-ordinate system. The force acting on the rotor can be described as given by Eq. 1 (see *nomenclature,* after the list of references, for symbol definitions). This force is determined for both orthogonal directions, as denoted by the *x* and *y* subscripts.

$$F = 0 \quad if \quad R_{rotor} < R_{airgap}$$

$$F = \sqrt{\left[K\cdot(x-ag_x)+C\cdot\frac{d(x-ag_x)}{dt}\right]^2+\left[K\square y-ag_y\ +C\frac{d(y-ag_y)}{dt}\right]^2} \quad if \quad R_{rotor} \geq R_{airgap} \tag{1}$$

with $R_{rotor} = \sqrt{x^2+y^2}$, $ag_x = R_{airgap} \times \frac{x}{R_{rotor}}$ and $ag_y = R_{airgap} \times \frac{y}{R_{rotor}}$.

2.2. Stator modelling

The stator is modelled using dampers, stiffnesses and masses. The differential equations are given by Eq. 2, Eq. 3 and Eq. 4 respectively.

$$F = K\cdot x \tag{2}$$
$$F = C\cdot v = C\cdot\dot{x} \tag{3}$$
$$F = M\cdot\alpha = M\cdot\dot{v} = M\cdot\ddot{x} \tag{4}$$

The stator is then modelled using these basic elements as shown in Fig. 2. It can clearly be seen that the rotor is not modelled as only a mass but rather as a rotor-model. The rotor model has as inputs, the force exerted at the AMB and BB locations, and as outputs the position at the AMB-sensor and BB locations. Thus the BB/stator model determines the force exerted on the rotor for a certain displacement and velocity. This force is then fed towards the rotor model that determines the position of the rotor for that particular force, velocity and rotational speed of the rotor.

2.3. Rotational backup bearing sub-model.

This model focuses on the bearing/rotor contact friction. Some of these effects couple directly back to the translational BB model and will be explained in detail. The rotational model is shown in Fig. 1.

Friction (rotor on inner race). The friction model used in the RDSim is a standard Coulomb friction model shown in Eq. 5. Coulomb friction is independent of the relative speed of the contacting surfaces. As long as there is relative motion, the friction force is proportional to the normal force.

$$\begin{aligned} F_{friction} &= F_{normal} \cdot \mu_{SteelOnSteel} \quad if \quad v_{relative} \neq 0 \\ F_{friction} &= 0 \quad if \quad v_{relative} = 0 \end{aligned} \tag{5}$$

The normal force experienced by the rotor is simply the vector sum of the forces in each of the orthogonal directions. The friction force is tangential to the contact point and in the opposite direction as the rotational direction as shown in Fig. 1. The friction force can be transposed to the midpoint of the rotor by transforming the force into a force-couple pair.

The friction force couples the orthogonal directions of the translational BB model. The normal force in each direction is perpendicular to each other. This means that the friction force in the *X* direction influences the total force in the *Y* direction. The relationship between the friction forces is given by Eq. 6.

$$\begin{aligned} F_{friction_X} &= F_{normal_Y} \cdot \mu_{SteelOnSteel} \quad , \quad F_{friction_Y} = F_{normal_X} \cdot \mu_{SteelOnSteel} \\ F_{Total_X} &= F_{normal_X} + F_{normal_Y} \cdot \mu_{SteelOnSteel} \quad , \quad F_{Total_Y} = F_{normal_Y} + F_{normal_X} \cdot \mu_{SteelOnSteel} \end{aligned} \tag{6}$$

The friction force determined using the normal force in the x direction is added to the translational BB model in the y direction and vice versa. This couples the orthogonal axes so that forces experienced in one direction influences the behaviour of the rotor in the other direction. This is graphically shown in Fig. 3. Should the surface speeds of the rotor and the inner race of the BB be equal the friction force is zero. The surface speeds are given by Eq. 7.

$$v_{rotor} = \omega_{rotor} \cdot R_{rotor} \quad , \quad v_{innerRace} = \omega_{innerRace} \cdot R_{innerRace} \tag{7}$$

The equations for the total force experienced are therefore dependent on the relative speed of the rotor and the bearing inner-race given by Eq. 8. It has to be noted that when the rotor speed is less than the inner-race speed, all of the friction forces change direction.

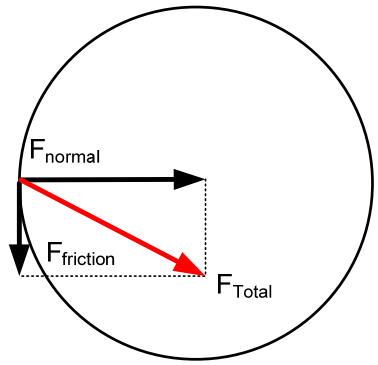

Fig. 3: Total force on rotor

$$\begin{aligned} &\text{if } \left[v_{rotor} - v_{innerRace} \neq 0 \right] \text{ then} \\ &F_{Total_X} = F_{normal_X} + F_{normal_Y} \cdot \mu_{SteelOnSteel} \\ &F_{Total_Y} = F_{normal_Y} + F_{normal_X} \cdot \mu_{SteelOnSteel} \\ &\text{if } \left[v_{rotor} - v_{innerRace} = 0 \right] \text{ then} \\ &F_{Total_X} = F_{normal_X} \, , \quad F_{Total_Y} = F_{normal_Y} \end{aligned} \tag{8}$$

Eq. 8 implies that the rotor will experience a force compelling it to move in the direction perpendicular to the normal force until the bearing inner race and the rotor have the same surface speeds at which point the rotor will only experience the reaction force to the normal force.

Inner-race acceleration and rotor deceleration. While the rotor and bearing are in contact the bearing speeds up to the rotor speed. When the rotor and bearing are not in contact the bearing will decelerate according to the bearing friction. The acceleration of the inner-race is calculated using Eq. 9.

$$\alpha_{innerRace} = \frac{\tau}{I_{innerRace\&Balls}} = \frac{F_{totalFriction} \cdot R_{innerRace}}{I_{innerRace\&Balls}} = \frac{\sqrt{F_{Normal_x}^2 + F_{Normal_y}^2} \cdot \mu \cdot R_{innerRace}}{I_{innerRace\&Balls}} \tag{9}$$

The braking of the rotor due to the contact is calculated in a similar way, but is opposite in direction (and is usually very small due to the fact that the rotor moment of inertia is a lot larger than the inner race and balls' moment of inertia). The relationship for the deceleration of the rotor is given in Eq. 10.

$$\alpha_{rotor} = \frac{-\tau}{I_{rotor}} = \frac{-\sqrt{F_{Normal_x}^2 + F_{Normal_y}^2} \cdot \mu \cdot R_{rotor}}{I_{rotor}} \tag{10}$$

The bearing rolling friction is dependent on bearing parameters. The calculation of the rotor deceleration, caused by bearing rolling friction, is given by Eq. 11 [12].

$$\alpha_{bearing_{friction}} = -\left[\frac{F_{total} + F_{preload}}{C_{static}}\right]^{\frac{1}{3}} \cdot \frac{Z \cdot \left(F_{total} + F_{preload}\right) \cdot D_{mean_{bearing}}}{I_{innerRace\&balls}} \tag{11}$$

If the rotor is actively braked (e.g. by a resistor bank) the rotor has a constant braking torque applied to it. The formula for this is shown in Eq. 12.

$$\alpha_{rotor_{brake}} = \frac{-\tau_{brakingtorque}}{I_{rotor}} \tag{12}$$

With all the accelerations known, the total acceleration and deceleration of the inner-race and rotor can be determined as given by Eq. 13.

$$\alpha_{Bearing_{total}} = \alpha_{innerRace} + \alpha_{bearing_{friction}} \quad , \quad \alpha_{Rotor_{total}} = \alpha_{rotor} + \alpha_{rotor_{brake}} \tag{13}$$

The rotor and the bearing both have an initial speed (usually the rotor is at operating speed and the bearing speed is 0). The rotational speed losses at that particular time-step are subtracted from the initial rotational speed.

The determined rotational speed of the rotor is fed back to the rotor model and is used as the rotational speed of the next timestep. The rotational speed of the BBs is used to determine the friction force and the direction of the friction force.

2.4. The active magnetic bearing sub-model

The AMB model is based on the model in [5] but simplified to ease the computational intensity of the RDSim. The AMB model as shown in Fig. 4 is only representative of the bearing stiffness and damping. A representation of the model for one axis of one AMB is shown in Fig..

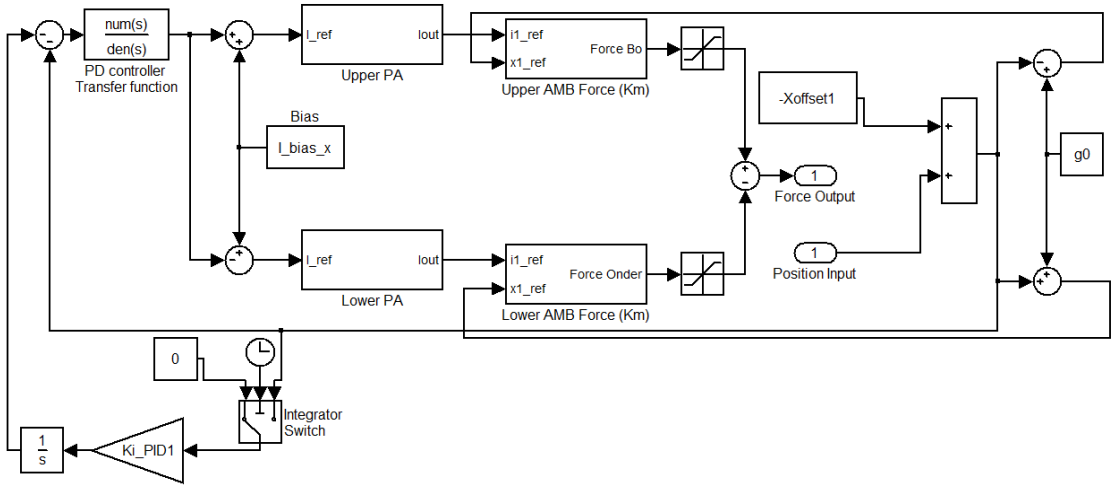

Fig.4: The AMB model

To explain the operation of the AMB model start at the position input to the model (refer to Fig.). If the rotor is to be levitated off-centre an offset value is assigned to "-Xoffset1" (shown in Fig. 4) and is added to the position reference. The position reference is fed to the PD controller. The PD controller calculates a reference current; the bias current is added to and subtracted from this reference current to obtain revised reference currents for the upper and lower coils of the AMB. The reference current is fed to the PA block. The PA is once again represented using a transfer function. The PA block determines the true current that the PA delivers for that specific reference current. The current is transformed into a force using Eq. 14.

$$F_{upper} = \frac{K_m \cdot i_{upper}^2}{x_{upper}^2} \quad , \quad F_{lower} = \frac{K_m \cdot i_{lower}^2}{x_{lower}^2} \quad , \quad F_{resultant} = F_{upper} - F_{lower} \tag{14}$$

The resultant force is determined by subtracting the lower force from the upper force. The resultant AMB force is the output of the AMB model.

2.5. Rotor sub-model

The rotor model used in the BBSim model is based on the RotFE code that was made available by I. Bucher [4]. The rotor in question is modelled using RotFE. RotFE determines the state space equation of the rotor. The state-space model is derived for each timestep during simulation, to account for changes in rotational speed. The rotor model will not be discussed in great detail. Only the changes made to the standard RotFE [4] code and the coupling of the rotor model is discussed. An example of a rotor is shown in Fig. 5. The position sensors (on the physical system) are not in the same location as the AMBs thus the measurement of the position is not accurate for bending modes, and conical modes. Therefore the BBSim model should also incorporate the non-collocation of the sensors and AMBs. The AMB controller uses the position data measured at the sensor locations and applies force at the AMB locations. In Table 1 the rotor model inputs and outputs are given

and the source of the input is also related. The destination of the output is also given. Table should be read while referring to Fig. 5. The rotor model determines the position of each of the nodes in the rotor model.

Table 1: Rotor model input and output

Rotor model inputs		Rotor model outputs	
Designation	Origin	Designation	Destination
Rotor rotational speed	BB rotational and friction model	Rotor position @ AMB sensor locations	AMB model
AMB force	AMB model		
BB force	BB translational model and friction model	Rotor position @ BB locations	BB translational model
Gravity force	BB translational model		

2.6. Coupling of the sub-models

The sub-models discussed in the paper are all interconnected. This section will explain how and to what each of these models is coupled. The coupling of each of these sub-models is shown in Fig. 6.

The translational BB models receive the current position of the rotor from the rotor model. The BB model also receives the friction force from the friction model determined from the

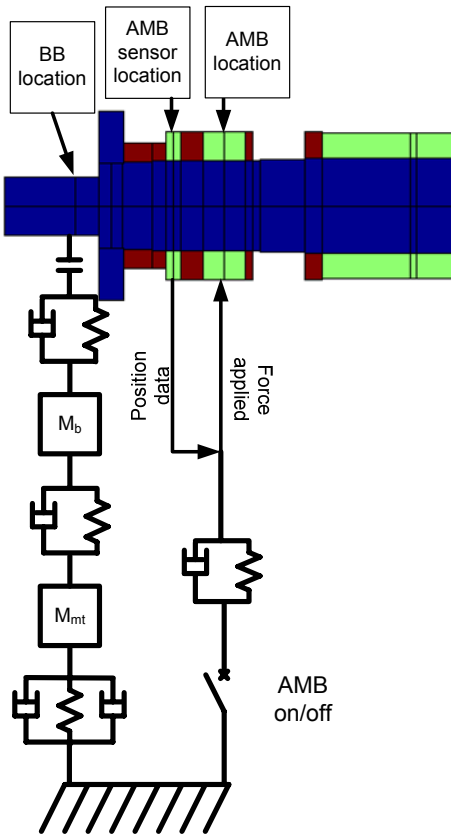

Fig. 5: Rotor model with AMB sensor and force locations

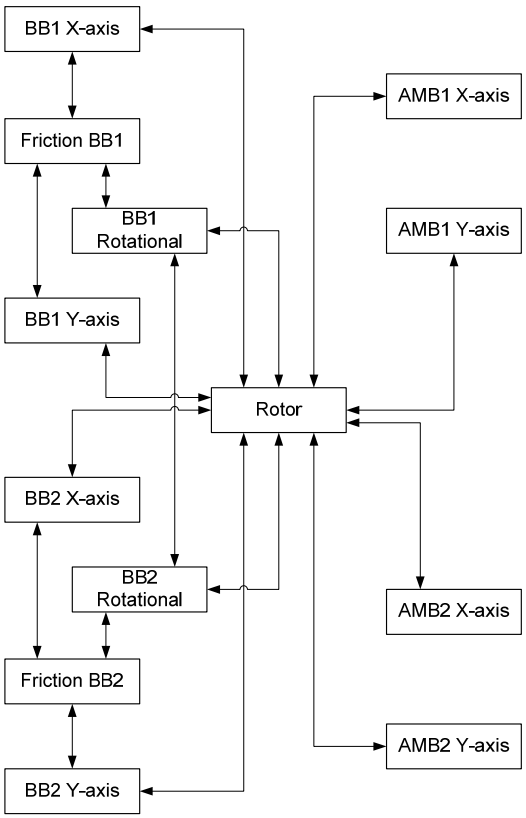

Fig. 6: Sub-model coupling

normal force on the other axis.

The BB model also delivers the force determined in each to the rotor model. The friction model receives the normal forces acting on the rotor and uses them to determine the friction

forces. It also receives the current bearing speed from the rotational BB model and sends the current friction factor to the rotational model.

The rotational BB model receives the perpendicular forces from the friction model and determines the speed-up torque of the bearing and the slow-down torque of the rotor. It also receives the current friction factor from the friction model.

The AMB model receives the current position of the rotor at the sensor locations, and sends the forces acting on the rotor at the AMB locations.

The rotor model receives the forces acting on the rotor (from AMBs and BBs) and sends the current position of the rotor (to the AMBs and BBs). It receives the current rotational speed from the rotational BB model.

3. Simulated results

Results obtained using RDSim to simulate a 4-axis controlled AMB suspended flexible rotor [10]. The AMBs are turned off at 10e-3 seconds. The orbital plots of the Rotor at the BB locations and the centre of mass of the rotor is shown in Fig. 7. In the centre of mass orbital plot shown below it can be seen that the rotor bends because the displacement is greater than at the bearing locations.

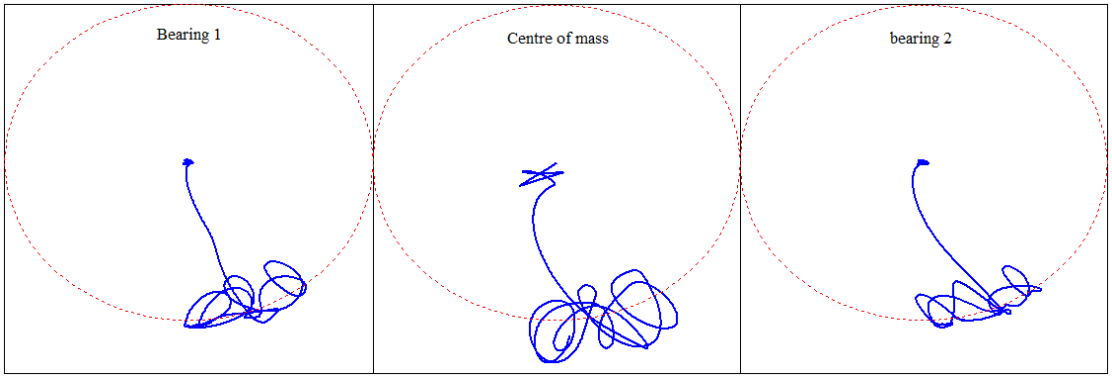

Fig. 7: Orbital plot of rotor centre at bearing locations and centre of mass

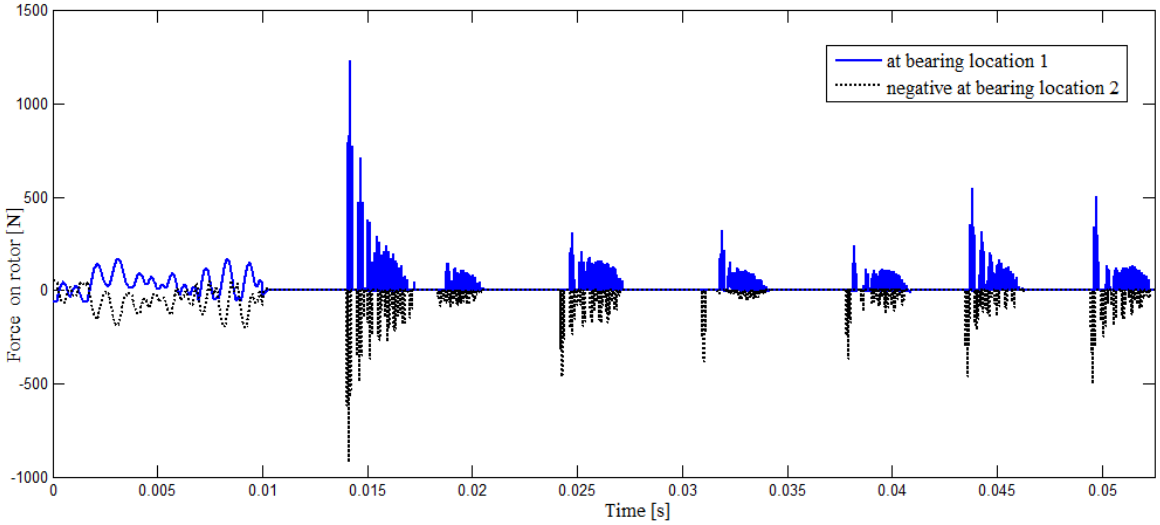

Fig. 8: Force at bearing locations

Fig. 8 shows the force experienced by the rotor at the two BB locations. The force due to magnetic decay can be seen in Fig. 9. Fig. 10 shows the two BB inner race speed-up and the deceleration of the rotor due to contact and bearing friction.

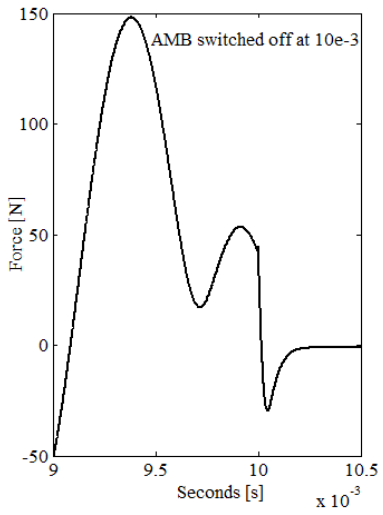

Fig. 9: Magnetic decay

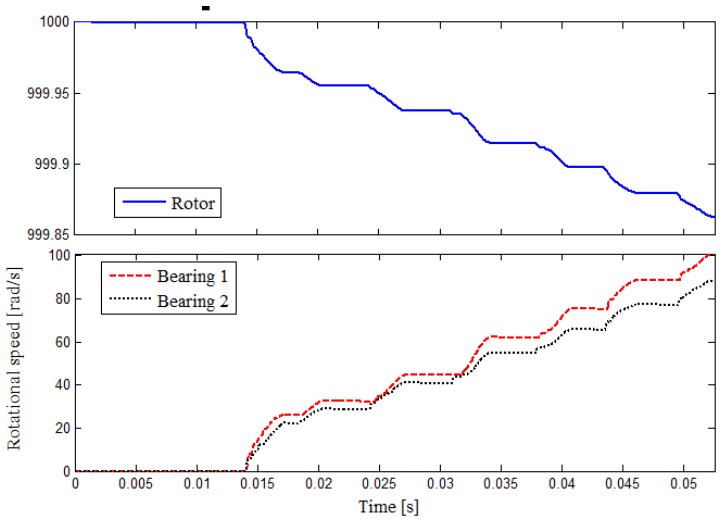

Fig. 10: Rotational speed of rotor and races

4. Future work and conclusion

Future work on the BBSim includes the verification of the rotor model on a high-speed (30 000 rpm) [13] rotor running on normal rolling element bearings. The verification of the backup bearing model on a 4 axis suspended AMB/BB system [10] and a 5 Axis suspended AMB/BB system [11]. An investigation into the causes of forward whirl still needs to be completed.

The BBSim model and sub-models were described and successfully integrated into a working backup bearing simulation model including various cross-coupled effects.

5. References

[1] Y. A. Amer and U. H. Hegazy, "Resonance Behaviour of a Rotor-Active Magnetic Bearing with Time-Varying Stiffness," Chaos, Solitons & Fractals, vol. 34, pp. 1328-1345, 2007.

[2] H. Ming Chen, James Walton, and Hooshang Heshmat, "Zero clearance auxiliary bearings for magnetic bearing systems," in ASME Tubo Expo, 1997.

[3] E. N. Cuesta, V. R. Rastelli, L. U. Medina, N. I. Montbrun, and S. E. Diaz, "Non-Linear Behaviours in the Motion of a Magnetically Supported Rotor on the Catcher Bearing During Levitation Loss, an Experimental Description," in ASME Turbo Expo, 2002, pp. 3-6.

[4] Izhak Bucher, "RotFE 2.1 The Finite Element Rotor Analysis Package," Faculty of mechanical Engineering, Technion, Haifa, user manual 2000.

[5] Stefan Myburgh, "A Non-linear Simulation Model of an Active Magnetic Bearings Supported Rotor System," in International Conference on Electrical Machines, Rome, Italy, 2010.

[6] J. Schmied and J. C. Pradetto, "Behaviour of a One Ton Rotor Being Dropped Into Auxiliary Bearings," in Proceedings of the Third International Symposium on Magnetic Bearings, Alexandria, Virginia, USA, 1992.

[7] Matthew T. Caprio, Brian T. Murphy, and John D. Herbst, "Spin Commissioning and Drop Tests of a 130 kW-Hr Composite Flywheel," in The Ninth International Symposium on Magnetic Bearings, Lexington, Kentucky, USA, 2004, pp. 3-6.

[8] Lawrence Hawkins, Alexei Filatov, Shamim Imani, and Darren Prosser, "Test Results and Analytical Predictions for Rotor Drop Testing of an Active Magnetic Bearing Expander/Generator," Transactions of the ASME, vol. 129, pp. 522-529, 2007.

[9] David Ransom, Andrea Masala, Jeffrey Moore, Giuseppe Vannini, and Massimo Camatti, "Numerical

and Experimental Simulation of a Vertical High Speed Motorcompressor Rotor Drop onto Catcher Bearings," in 11th International Symposium on Magnetic Bearings, Nara, Japan, 2008, pp. 136-143.

[10] Eugén Otto Ranft, "The development of a flexible rotor active magnetic bearing system," North West University, Potchefstroom, Masters thesis 2005.

[11] Nico-Johan Besinger, "The adaption of a rotor for active magnetic bearing levitation and the corresponding auxiliary bearing design," North-West University, Potchefstroom, South Africa, Masters thesis 2009.

[12] T A Harris and M N Kotzala, Rolling Element Bearing Analysis, Advanced concepts of bearing technology, 5th ed. Boca Raton, United States of America: CRC Taylor & Francis press, 2007.

[13] C J G Ranft, "Stress in a multi-ring high speed rotor of a permanent magnet synchronous machine," North-West University, Potchefstroom, South Africa, Dissertation 2008.

Nonmenclature

R	Radius (radial position)	R_{rotor}	Radius to rotor mid-point from origin
F	Force	R_{airgap}	Radius to airgap from origin
K	Stiffness coefficient	$\mu_{SteelOnSteel}$	Friction factor of steel on steel
K_m	Magnetic Stiffness	i	electrical current
C	Damping coefficient	Z	number of rolling elements in bearing
C_{static}	Static bearing load rating	D	Diameter
ag	Air gap	I	Moment of inertia
x	Position along x-axis	τ	Torque
y	Position along y axis	ω	Angular velocity
M	Mass	μ	Friction factor
α	Acceleration/deceleration	v	Surface speed